JPET Fast Forward. Published on May 27, 2004 as DOI: 10.1124/jpet.104.069930

JPET #69930

The N-methyl-D-aspartate Receptor Inhibitory Potencies of Aromatic Inhaled Drugs of Abuse: Evidence for Modulation by Cation-π Interactions

Douglas E. Raines, Fredrick Gioia, and Robert J. Claycomb, Renna J. Stevens

Department of Anesthesia and Critical Care, Massachusetts General Hospital, Boston, MA

JPET #69930

Running title: Inhibition of NMDA Receptors by Aromatic Inhalants

Address Correspondence to: Douglas E. Raines, Department of Anesthesia and Critical Care, Massachusetts General Hospital, 55 Fruit Street, Boston, MA 02114

Tel: (617) 724-0343, Fax: (617) 724-8644

Email: draines@partners.org

Tables: 1

Figures: 6

References: 48

Words in abstract: 182

Words in introduction: 583

Words in discussion: 1518

Abbreviations: NMDA, N-methyl-D-aspartate; $GABA_A$, γ-aminobutyric acid type A; tricaine, ethyl-m-aminobenzoate

Recommended Section Assignment: Neuropharmacology

Abstract

Benzene and several close structural analogues are inhaled drugs of abuse with general anesthetic activity. By virtue of their π electron clouds, they may engage in attractive electrostatic interactions with cationic atomic charges on protein targets. In this study, we tested the hypothesis that inhaled drugs of abuse inhibit human N-methyl-D-aspartate (NMDA) receptors with potencies that correlate with their abilities to engage in cation-π interactions. Electrophysiological techniques were used to define the NR1/NR2B NMDA receptor inhibitory concentrations of volatile benzene analogues and computer modeling was used to quantify their abilities to engage in cation-π interactions and their molecular volumes. In addition, each compound's octanol:gas partition coefficient (a measure of hydrophobicity) was quantified. All 18 compounds inhibited human NR1/NR2B NMDA receptors reversibly and in a concentration-dependent manner. NMDA receptor inhibitory potency correlated strongly with the ability to engage in cation-π interactions, weakly with hydrophobicity, and was independent of molecular volume. This is consistent with the hypothesis that cation-π interactions enhance the binding of inhaled drugs of abuse to the NMDA receptor and suggests that the receptor binding site(s) for these drugs possesses significant cationic character.

Introduction

More than a century ago, Meyer and Overton observed that compounds induce anesthesia with potencies that correlate strongly with their oil solubilities, implying that hydrophobic interactions are the major determinants of anesthetic potency (Meyer, 1899; Overton, 1901). This correlation, termed the Meyer-Overton Correlation, is most commonly interpreted to mean that anesthetics induce anesthesia via interactions with hydrophobic protein domains, a view supported by numerous studies demonstrating that anesthetics alter the function of proteins with potencies that correlate strongly with both their hydrophobicities and *in-vivo* anesthetic potencies (Firestone et al., 1994; Mihic et al., 1994; Raines et al., 2002; Wood et al., 1991; Zimmerman et al., 1994). However, it has been suggested that other interactions also make important contributions towards defining anesthetic potency (Eckenhoff and Johansson, 1997; Johansson and Zou, 1999). In particular, electrostatic interactions (e.g. hydrogen bonding interactions) between anesthetics and their receptor targets have recently been suggested to modulate the agonist-enhancing actions of anesthetics on $GABA_A$ and nicotinic acetylcholine receptors and the inhibitory actions of anesthetics on firefly luciferase (Abraham et al., 1991; Moss et al., 1991; Raines et al., 2001; Raines et al., 2003).

Volatile aromatic compounds such as benzene and toluene are found in a variety of household and commercial products where they are commonly used as solvents or as major components of adhesives and cleaning fluids. Some may also be inhaled to produce dizziness, learning and memory impairment, and even unconsciousness and, thus, are general anesthetics (Balster, 1998; Fang et al., 1996; Massey and Jackson, 1973; Neal and Robson, 1966). By virtue of their π electrons, these inhalants may engage in

electrostatic interactions with protein residues that possess cationic atomic charge (Mecozzi et al., 1996). Such interactions (cation-π interactions) can have strengths that are comparable to or stronger than that of a typical hydrogen bond (several kcal/mol) and have become increasingly recognized as an important molecular force contributing to the binding of ligands to receptor targets (Beene et al., 2002; Manderson and Johansson, 2002; Watts, 2002; Zacharias and Dougherty, 2002; Zhong et al., 1998). Consequently, cation-π interactions may be important determinants of the receptor potencies of volatile aromatic inhalants.

The NMDA receptor is a calcium-permeable ligand-gated ion channel that mediates excitatory synaptic transmission in the brain. It is thought to play an important role in synaptic plasticity, memory and motor coordination and has been implicated in a number of pathologic conditions including Alzheimer's and Parkinson's diseases, Huntington's chorea, schizophrenia, and epilepsy (Chase et al., 2000; Coyle et al., 2002; Kemp and McKernan, 2002). The NMDA receptor is also considered to be an important target of a number of inhaled and non-inhaled anesthetics such as nitrous oxide, xenon, cyclopropane, ethanol and ketamine that dose-dependently and reversibly inhibit NMDA receptor mediated currents at physiologically relevant concentrations (Peoples and Weight, 1995; Peoples et al., 1997; Raines et al., 2001; Yamakura and Harris, 2000). Benzene and alkylbenzenes also potently inhibit NMDA receptor function and induce anesthesia, suggesting that aromatic inhalants may produce their physiological effects, at least in part, by inhibiting NMDA receptor function (Cruz et al., 2000; Cruz et al., 1998).

The purpose of this study was to test the hypothesis that cation-π interactions are important molecular forces governing the NMDA receptor inhibitory potencies of volatile

aromatic inhalants. We used electrophysiological techniques to define the NMDA receptor inhibitory potencies of volatile aromatic inhalants and quantified each inhalant's octanol:gas partition coefficient (a measure of anesthetic hydrophobicity) experimentally and cation-π binding energy and molecular volume computationally for use as molecular descriptors for structure-activity analysis.

Materials and Methods

Determination of Solvent:Gas Partition Coefficients (table 1)

Buffer:Gas Partition Coefficient. For each inhalant, a stock solution of buffer containing inhalant (0.05 –1 mM) was prepared. Three to seven mL of stock solution was added to a calibrated gas-tight 10-mL syringe via a 3-way stopcock. Room air (gas) was added to the syringe to bring the total volume of buffer and gas to 10 mL and the stopcock was closed. The stock solution and gas were shaken for 1-2 hours at room temperature (20-22°C) to reach equilibrium. The concentrations of inhalant in the stock solution before and after equilibration with gas were determined spectrophotometrically.

The partition coefficient (λ) was calculated as:

$$\lambda = \frac{V_{gas}}{V_{stock}} \cdot \frac{C_2}{(C_1 - C_2)} \qquad \text{equation 1}$$

where V_{gas} and V_{stock} are the volumes of gas and stock solution, respectively, in the syringe, C_1 and C_2 are the inhalant concentrations of the stock solution before and after, respectively, equilibration with gas.

*Octanol:Gas Partition Coefficient*s. For each inhalant, a stock solution of octanol containing inhalant (0.05 –1 mM) was prepared. Two mL of stock solution was added to a 2 L glass bottle that was immediately sealed with a teflon-coated cap. The stock solution and gas were shaken at room temperature for 1-2 hours to reach equilibrium. The concentrations of inhalant in the stock solution before and after equilibration with gas were determined as described above and the octanol:gas partition coefficient was calculated using equation 1.

Molecular Modeling

An electrostatic potential map for each inhalant was generated and cation-π binding energy calculated using MacSpartan Pro V1.01 (Wavefunction Inc., Irvine, CA) on an Apple MacIntosh G4 computer. Geometry optimization was performed using *ab initio* molecular orbital calculations (Hartree-Fock, 6-31G** basis set). The cation-π binding energy was defined as the negative binding energy of a generic cation probe (Na^+) to the inhalant's π electron cloud as previously described (Mecozzi et al., 1996). Molecular volumes were similarly obtained from *ab initio* molecular orbital calculations.

Oocyte Expression

Xenopus frogs were maintained and treated in accordance with regulations specified by the Massachusetts General Hospital Animal Care Committee (Boston, MA). Prior to surgery, frogs were anesthetized with 0.2% tricaine (ethyl-m-aminobenzoate) and hypothermia. Ovary lobes were excised via a small laparotomy incision and placed in OR-2 solution (in mM: 82 NaCl; 2 KCl; 1 MgCl2, 5 Hepes; pH 7.6). Following a 1 hour incubation period in collagenase D (1 mg/ml in OR-2) to separate oocytes from connective tissue, stage 4 and 5 oocytes were selected for injection with mRNA encoding the NR1 and NR2B subunits of the NMDA receptor. Oocytes were injected with 5-10 ng of mRNA encoding for each subunit at a ratio of 1:1 and incubated in microtiter wells for at least 24 hours in ND-96 buffer (in mM: 96 NaCl; 2 KCl; 1 CaCl2, 0.8 MgCl2; 10 Hepes; pH 7.6) containing 5 u/ml of penicillin and 5 µg/ml of streptomycin at 17°C prior to electrophysiological studies.

Electrophysiology

All experiments were performed at room temperature. Oocytes were placed in a 0.04 ml chamber and impaled at the animal pole with two capillary glass electrodes filled with 3 M KCl and possessing open tip resistances of 0.2-2 MΩ. Oocytes were voltage clamped at –50 mV using a GeneClamp 500B amplifier (Axon Instruments, Foster City, CA). Oocytes were perfused with buffer (96 mM NaCl, 2 mM KCl, 2 mM $BaCl_2$, 10 mM Hepes, pH 7.6) at a rate of 4 ml/min. Buffer perfusion was controlled using a six channel valve controller (Warner Instr., Hamden, CT), interfaced with an Axon Digidata card, and driven by a personal computer using Axon's pClamp 8.0 software. The perfusion apparatus was made from gas-tight glass syringes and Teflon tubing to minimize absorptive and evaporative loss of inhalants. In parallel experiments, gas chromatographic analysis of solutions exiting the perfusion system and entering the oocyte chamber indicated that such loss was < 15%. Inhalants were purchased from Aldrich Chemical Co (Milwaukee, WI). NMDA and glycine was from Sigma Chemical Co. (St. Louis, MO).

In each experiment, a control current was first obtained by perfusing the oocyte with buffer containing 100 NMDA (+ 10 μM glycine) for 30 sec and measuring the peak current response. The effect of inhalant was then assessed after a 5 min recovery period by perfusing the oocyte with buffer containing inhalant for 60 sec and then switching to buffer containing inhalant and 100 NMDA (+ 10 μM glycine) for 30 sec and measuring the peak current response. After another 5 min recovery period, the control current was measured again to assure reversibility. The control peak current was quantified as the average of the two control experiments.

Data Analysis

Aqueous inhalant concentrations were converted to partial pressures using buffer:gas partition coefficients. Concentration-response curves were generated by plotting the peak current in the presence of anesthetic normalized to that in its absence (control). Each data point on all curves represents the mean of at least 3 measurements obtained using different oocytes and the error bars indicate the standard deviation from the mean. Data points were fit to a Hill equation using Igor Pro 4.01 (Wavemetrics Inc, Lake Oswego, OR) in the form:

$$I_{peak} = \frac{IC_{50}^{n}}{IC_{50}^{n} + [Drug]^{n}} \qquad \text{equation 2}$$

where I_{peak} is the normalized peak current in the presence of inhalant, IC_{50} is the concentration of inhalant that reduces the peak current by one-half, and n is the Hill coefficient.

Results

All 14 volatile aromatic inhalants inhibited NMDA-elicited currents reversibly and in a concentration-dependent manner. Representative traces demonstrating current inhibition by benzene, 1,3,5-trifluorobenzene, and perfluorobenzene are shown in figures 1A, 1B, and 1C respectively. In each figure, the first and last traces are the control currents recorded upon pulsing *Xenopus* oocytes expressing NR1/NR2B NMDA receptors with agonist. The middle trace demonstrates the NMDA receptor inhibitory actions of 3 x 10^{-3} atm benzene (1A), 6.1 x 10^{-2} atm 1,3,5-trifluorobenzene (1B) or 7.8 x 10^{-2} atm perfluorobenzene (1C) when applied prior to and during the agonist pulse. The concentration-response curves for NMDA receptor inhibition by these three inhalants are shown in figure 1D. At the highest concentrations studied, benzene and 1,3,5-trifluorobenzene inhibited nearly all of the agonist-elicited current (90 ± 3% and 94 ± 2%, respectively) whereas perfluorobenzene inhibited only 47 ± 6% of the current even at the highest attainable concentration (i.e. saturation). A fit of the data in figure 1D to equation 1 yielded IC_{50}s for benzene, 1,3,5-trifluorobenzene, and perfluorobenzene of 1.1 ± 0.1 x 10^{-3} atm, 5.1 ± 0.5 x 10^{-3} atm and 9.2 ± 0.8 x 10^{-2} atm, respectively. The respective Hill coefficients derived from these fits were 1.2 ± 0.1, 1.0 ± 0.1, and 0.75 ± 0.04.

Table 1 lists the NMDA receptor IC_{50}'s, Hill coefficients, and partition coefficients of all 14 volatile aromatic inhalants evaluated in this study. IC_{50}s ranged from 5.6 ± 0.3 x 10^{-4} atm (toluene) to 9.2 ± 0.8 x 10^{-2} atm (perfluorobenzene), a range of 164-fold and the Hill coefficients averaged 0.94 ± 0.22. The hydrophobicities of these inhalants, as reflected by their octanol:gas partition coefficients ($\lambda_{octanol:gas}$), ranged from

JPET Fast Forward. Published on May 27, 2004 as DOI: 10.1124/jpet.104.069930
This article has not been copyedited and formatted. The final version may differ from this version.

389 ± 9 (perfluorobenzene) to 8430 ± 400 (m-xylene). Where hydrophobicity is the principle determinant of inhibitory potency, then log ($1/IC_{50}$) and log ($\lambda_{octanol:gas}$) are predicted to be strongly correlated. Although the regression analysis of our data revealed that the correlation between log ($1/IC_{50}$) and log ($\lambda_{octanol:gas}$) reached statistical significance ($p = 0.044$), it also indicated that inhalant hydrophobicity was a relatively poor predictor of NMDA receptor inhibitory potency (r^2=0.30; figure 2A).

Previous studies have shown that general anesthetics act on many protein targets, including the NMDA receptor, with potencies that depend upon their size (Jenkins et al., 2001; Mascia et al., 1996; Peoples and Ren, 2002; Peoples and Weight, 1995; Wick et al., 1998; Wood et al., 1993). Commonly, potency increases with anesthetic molecular volume because molecular volume often correlates with hydrophobicity (Abraham et al., 1991). However in some cases, the potencies of larger, more hydrophobic anesthetics are less than would be predicted from the extrapolation of the potencies of smaller, less hydrophobic ones (a phenomenon termed "cutoff"), presumably because steric hindrance reduces anesthetic binding to a site that is limited in size. In our group of inhalants, we observed no relationship between inhalant molecular volume and NMDA receptor inhibitory potency (table 1). For example, although perfluorobenzene's molecular volume is not different from those of ethylbenzene and the three xylene isomers (~119Å^3), its potency is approximately 2 orders of magnitude lower. Similarly, while benzene has the smallest molecular volume (86.6 Å^3) and ethylbenzene has one of the largest volumes (119.8 Å^3), their NMDA receptor inhibitory potencies are not different (1.1×10^{-3} atm.). Figure 2B plots log ($1/IC_{50}$) versus molecular volume for the entire

group of aromatic inhalant to demonstrate the lack of correlation between the inhibitory potencies and molecular volumes of the inhalants studied ($p= 0.19$, $r^2=0.14$).

Using quantum mechanical modeling, we also characterized the electrostatic potential surfaces of these inhalants and quantified their abilities to engage in cation-π interactions (figure 3). In this figure, we used a color scale ranging from +20 to –20 kcal/mol to emphasize the electrostatic potential differences in the aromatic ring regions. Blue was used to signify an electrostatic potential equal to or more positive than +20 kcal/mol and red to indicate a potential equal to or more negative than –20 kcal/mol. Inspection of this figure reveals that the electrostatic potential surfaces of these inhalants vary greatly. Benzene and its alkyl-substituted analogues possess regions of highly negative electrostatic potential over their aromatic rings, reflecting the high electron density of their π systems. Because fluorine groups withdraw electron density, the successive addition of fluorine onto the aromatic ring progressively reduces the negative electrostatic potential of the π system and, thus, the ability to engage in cation-π interactions.

Benzene and its five alkyl-substituted analogues possess similarly high abilities to engage in cation-π interactions (29 ± 1 kcal/mol; figure 3) and similarly low NMDA receptor IC_{50}s ($1.0 \pm 0.5 \times 10^{-3}$ atm; table 1). Conversely, perfluorobenzene can not engage in cation-π interactions and has an IC_{50} that is nearly two orders of magnitude higher than those of benzene and its alkyl-substituted analogues. Figure 4 plots log ($1/IC_{50}$) versus cation-π interaction strength and demonstrates that the relationship is linear and the correlation highly significant ($r^2 = 0.85$, $p < 0.0001$), suggesting that

attractive cation-π interactions are important determinants of NMDA receptor inhibitory potency.

We further explored the role that cation-π interactions might play in modulating NMDA receptor inhibitory potency using a second set of volatile compounds: cyclohexene, 1,4-cyclohexadiene, 4-methyl-1-cyclohexene, and 1-methyl-1,4-cyclohexadiene. These compounds are structurally similar to benzene and toluene, but vary in the extent of their π-electron system and, thus, their predicted abilities to engage in cation-π interactions. *Ab initio* molecular orbital calculations confirmed this prediction as the cation-π interaction strengths of these compounds in kcal/mol were 28.6 (toluene), 27.1 (benzene), 24.9 (1-methyl-1,4-cyclohexadiene), 24.2 (1,4-cyclohexadiene), 19.1 (4-methyl-1-cyclohexene) and 18.8 (cyclohexene). Electrophysiological studies revealed that all of these compounds reversibly inhibited NMDA receptor-mediated currents in a concentration-dependent manner. The inhibitory potencies ranged nearly 2 orders of magnitude and the relationship between log (IC_{50}) and the cation-π binding energy was linear and the correlation highly significant (figure 5A; $r^2 = 0.97$, $p = 0.0004$). Conversely, the potencies of these compounds did not correlate significantly with either their hydrophobicities ($r^2 = 0.22$, $p = 0.355$; figure 5B) or their molecular volumes ($r^2 = 0.14$, $p = 0.86$; figure 5C).

We then evaluated the dependence of NMDA receptor inhibitory potency on NMDA and glycine concentrations. We chose benzene (4.6×10^{-3} atm) and perfluorobenzene (0.11 atm) as representative aromatic inhalants having high and low inhibitory potency, respectively. Currents were measured upon activation by 100 μM NMDA and 10 μM glycine, 1000 μM NMDA and 10 μM glycine, or 100 μM NMDA

and 100 μM glycine. As shown in figure 6, 10-fold increases in either NMDA or glycine did not significantly reduce the inhibitory potencies of these inhalants, indicating that the inhalants do not inhibit NMDA receptors by competing with NMDA or glycine for binding.

Discussion

Clinical anesthetics and inhaled drugs of abuse representing a wide range of chemical classes including alkanes, ethers, and even noble gases may be inhaled to produce a constellation of behaviors (e.g. unconsciousness, amnesia, analgesia, and immobility in response to noxious stimulation) that are collectively referred to as the state of anesthesia (Fang et al., 1997; Koblin et al., 1998; Sonner et al., 1998; Zhang et al., 2000). Although the receptors responsible for the production of the anesthetic state are not known with certainty, the $GABA_A$, glycine, and NMDA receptors are generally considered to be among the most likely candidates (Franks and Lieb, 1994). The predominant actions of drugs with anesthetic activity are to enhance inhibitory $GABA_A$ and glycine receptor function and/or to inhibit excitatory NMDA receptor function (de Sousa et al., 2000; Hollmann et al., 2001; Mascia et al., 1996; Orser et al., 1997; Zimmerman et al., 1994).

Studies to define the relationship between the structure of anesthetic drugs and their receptor activities have commonly used members of the homologous series of normal alcohols (Peoples and Weight, 1995; Wick et al., 1998; Wood et al., 1991). In this series, alcohol hydrophobicity and molecular volume increase steadily with alkyl chain length, allowing one to readily assess the importance that hydrophobic and steric interactions play in modulating potency. In the NMDA receptor, inhibitory potency increases upon ascending the series from methanol to heptanol (Peoples and Weight, 1995). Cutoff is observed beyond heptanol as octanol is less potent than heptanol and the potencies of higher homologues are so low that even saturated solutions fail to produce

any detectable inhibition. Similarly in $GABA_A$ and glycine receptors, the potentiating actions of normal alcohols increase with alkyl chain length before reaching a cutoff between decanol and dodecanol, a pattern of activity suggesting that hydrophobic interactions enhance alcohol binding affinity and hence potency whereas steric interactions reduce them (Wick et al., 1998).

In addition to hydrophobic and steric interactions, electrostatic interactions between drugs and their protein targets have been proposed to be important forces modulating potency (Abraham et al., 1991; Eckenhoff and Johansson, 1997; Manderson and Johansson, 2002; Moss et al., 1991; Raines et al., 2003). Among the strongest electrostatic interactions that may occur between a volatile drug and a protein binding site are hydrogen-bonding and cation-π interactions. Hydrogen-bonding interactions may occur between a donor molecule that contains an "acidic" hydrogen and another molecule that contains an electronegative acceptor atom (most commonly oxygen or nitrogen in biological systems). A hydrogen atom is made acidic (i.e. develops a significant partial positive electrostatic charge) if it is bonded to an atom that also bonds electron-withdrawing groups. As many general anesthetics possess oxygen atoms (a hydrogen bond acceptor) and/or acidic hydrogen (a hydrogen bond donor), many anesthetics can hydrogen-bond to protein targets. Cation-π interactions are potentially strong attractive electrostatic interactions that occur between a π-electron cloud and an atom that carries a full or partial positive charge. Although none of the inhaled anesthetics currently used contain aromatic groups, a number of inhaled drugs of abuse with anesthetic activity do. Because hydrogen-bonding and cation-π interactions can provide several additional

kcal/mole of energy to stabilize protein binding, they can enhance the binding affinities of aromatic inhaled drugs by more than an order of magnitude.

Studies to examine the nature of the interactions modulating anesthetic binding to the firefly luciferase enzyme (a soluble protein model for studying such interactions) provide experimental support for the importance of electrostatic interactions (Abraham et al., 1991). These studies demonstrated that the enzyme's binding site for anesthetics, while possessing significant hydrophobic character, can accept a hydrogen bond from an anesthetic about as well as water can. Thus, anesthetics representing a range of chemical classes inhibit this enzyme with potencies that depend upon their hydrogen-bonding abilities. High resolution X-ray crystallographic studies of halogenated alkane binding to insulin dimers has provided direct structural evidence that favorable electrostatic interactions are strong enough to enhance binding affinity (Gursky et al., 1994). Manderson and Johansson showed that substituting tyrosine for tryptophan in a synthetic four-α-helix bundle reduces the binding affinity of the inhaled anesthetics chloroform and halothane 6- and 3-fold, respectively, without significantly changing the protein's overall structure (Manderson and Johansson, 2002). They concluded that interactions between the positive end of the anesthetic's dipole and the tryptophan's π-electron cloud enhances binding affinity. Similarly, high resolution NMR and photolabeling studies reveal that inhaled anesthetics can interact specifically with tryptophan residues in gramacidin A (Tang et al., 2000). However, Lui et al. were unable to detect such interactions between halothane and tryptophan in human serum albumin suggesting that the importance that cation-π interactions play in defining inhaled anesthetic binding

affinity varies with the target protein studied due to the specific physicochemical properties of the anesthetic binding site (Liu et al., 2002).

We have previously shown that electrostatic interactions can also modulate the potencies with which anesthetics act on ligand-gated ion channels. For example, general anesthetics enhance agonist action on *Torpedo* nicotinic acetylcholine receptors with potencies that correlate with their abilities to form hydrogen-bonds (Raines and Claycomb, 2002). Similarly, nonhalogenated alkanes, which are distinguished from most other anesthetics by their inability to engage in electrostatic interactions, enhance agonist action on $GABA_A$ receptors with potencies that are an order of magnitude lower than would be predicted by their hydrophobicities (Raines et al., 2003). However, electrostatic interactions do not seem to modulate anesthetic potency in all receptor systems as halogenated and nonhalogenated alkanes act on $\alpha_4\beta_2$ neuronal nicotinic acetylcholine receptors with potencies that correlate highly with their hydrophobicities and not their electrostatic properties (Raines et al., 2002).

In the present study, we tested the hypothesis that cation-π interactions can modulate the NMDA receptor inhibitory potencies of inhaled drugs of abuse. We used compounds whose abilities to engage in cation-π interactions vary depending upon either the identity of the substituent groups on the aromatic ring or the degree of conjugated unsaturation. The presence of strongly electron-withdrawing fluoro groups on aromatic rings or incomplete unsaturation substantially reduced the cation-π binding energy as determined by *ab initio* quantum mechanical calculations. Our studies reveal that volatile aromatic drugs inhibit NMDA receptor-mediated currents with potencies that are highly correlated with their abilities to engage in cation-π interactions. This is consistent with

an important role for cation-π interactions in modulating the inhibitory potencies of volatile aromatic compounds. Our findings also suggest that it is possible to predict the NMDA receptor inhibitory potencies of novel aromatic compounds using molecular modeling by defining their abilities to engage in cation-π interactions. Such an approach could lead to the rapid screening of available compounds or the design of new ones that inhibit NMDA receptors with high potency.

The compounds that we studied have NMDA receptor potencies that range by 164-fold (table 1). If this were due to differences in anesthetic binding affinity to the NMDA receptor, then this would represent a difference in binding energy between toluene and perfluorotoluene, the most and least potent anesthetics respectively, of 3.0 kcal/mol. This value is much lower than the binding energy calculated using molecular modeling which assumes that anesthetics interact with a full positive charge in a vacuum. It is, however, similar to the 2.4 kcal/mol and 4 kcal/mol values estimated for the cation-π interactions that modulate cationic agonist binding to a binding site tryptophan on nicotinic and serotonergic receptors, respectively (Beene et al., 2002). Solvation can reduce the effective cationic charge and, thus, the electrostatic contribution to the binding energy by a factor of 80 (based on the dielectric constant of 80 for water). The contribution to the binding energy may also be reduced if the cation-π interaction involves a partial cationic charge (i.e. the positive end of a permanent or inducible dipole) rather than a full charge.

We also assessed the contribution that anesthetic hydrophobicity and molecular volume make towards defining NMDA receptor inhibitory potency. For the 14 aromatic inhalants studied, the correlation between NMDA receptor inhibitory potency and

inhalant's hydrophobicity reached statistical significance, but it was not as strong as that observed between inhibitory potency and cation-π binding energy. Thus, hydrophobic interactions may explain the activity (albeit at very high concentrations) of perfluorbenzene which can not engage in cation-π interactions at all. For the second group of compounds in which the extent of conjugated unsaturation varies (fig. 5B), no significant correlation between NMDA receptor inhibitory potency and hydrophobicity was observed. Although there was some trend towards decreasing inhibitory potency with increasing molecular volume (figs. 2B and 5C), this trend was not statistically significant and cutoff at large molecular volume was not observed.

In summary, we used electrophysiological and computational approaches to assess the importance that cation-π interactions play in defining the NMDA receptor inhibitory potencies of inhaled drugs that possess π electrons. Our studies show that inhaled drugs inhibit NR1/NR2B NMDA receptors with potencies that are correlated strongly with their abilities to engage in cation-π interactions, weakly with their hydrophobicities, and are independent of their molecular volumes. This is consistent with the hypothesis that cation-π interactions enhance the binding of these inhaled drugs to the NMDA receptor and suggests that the binding site(s) for these drugs possesses significant cationic character.

References

Abraham MH, Lieb WR and Franks NP (1991) Role of hydrogen bonding in general anesthesia. *J Pharm Sci* **80**:719-724.

Balster RL (1998) Neural basis of inhalant abuse. *Drug Alcohol Depend* **51**:207-214.

Beene DL, Brandt GS, Zhong W, Zacharias NM, Lester HA and Dougherty DA (2002) Cation-pi interactions in ligand recognition by serotonergic (5-HT3A) and nicotinic acetylcholine receptors: the anomalous binding properties of nicotine. *Biochemistry* **41**:10262-10269.

Chase TN, Oh JD and Konitsiotis S (2000) Antiparkinsonian and antidyskinetic activity of drugs targeting central glutamatergic mechanisms. *J Neurol* **247 Suppl 2**:II36-42.

Coyle JT, Tsai G and Goff DC (2002) Ionotropic glutamate receptors as therapeutic targets in schizophrenia. *Curr Drug Target CNS Neurol Disord* **1**:183-189.

Cruz SL, Balster RL and Woodward JJ (2000) Effects of volatile solvents on recombinant N-methyl-D-aspartate receptors expressed in Xenopus oocytes. *Br J Pharmacol* **131**:1303-1308.

Cruz SL, Mirshahi T, Thomas B, Balster RL and Woodward JJ (1998) Effects of the abused solvent toluene on recombinant N-methyl-D-aspartate and non-N-methyl-D-aspartate receptors expressed in Xenopus oocytes. *J Pharmacol Exp Ther* **286**:334-340.

de Sousa SL, Dickinson R, Lieb WR and Franks NP (2000) Contrasting synaptic actions of the inhalational general anesthetics isoflurane and xenon. *Anesthesiology* **92**:1055-1066.

Eckenhoff RG and Johansson JS (1997) Molecular interactions between inhaled anesthetics and proteins. *Pharmacol Rev* **49**:343-367.

Fang Z, Ionescu P, Chortkoff BS, Kandel L, Sonner J, Laster MJ and Eger EI, 2nd (1997) Anesthetic potencies of n-alkanols: results of additivity and solubility studies suggest a mechanism of action similar to that for conventional inhaled anesthetics. *Anesth Analg* **84**:1042-1048.

Fang Z, Sonner J, Laster MJ, Ionescu P, Kandel L, Koblin DD, Eger EI, 2nd and Halsey MJ (1996) Anesthetic and convulsant properties of aromatic compounds and cycloalkanes: implications for mechanisms of narcosis. *Anesth Analg* **83**:1097-1104.

Firestone LL, Alifimoff JK and Miller KW (1994) Does general anesthetic-induced desensitization of the Torpedo acetylcholine receptor correlate with lipid disordering? *Molecular Pharmacology* **46**:508-515.

Franks NP and Lieb WR (1994) Molecular and cellular mechanisms of general anaesthesia. *Nature* **367**:607-614.

Gursky O, Fontano E, Bhyravbhatla B and Caspar DL (1994) Stereospecific dihaloalkane binding in a pH-sensitive cavity in cubic insulin crystals. *Proc Natl Acad Sci U S A* **91**:12388-12392.

Hollmann MW, Liu HT, Hoenemann CW, Liu WH and Durieux ME (2001) Modulation of NMDA receptor function by ketamine and magnesium. Part II: interactions with volatile anesthetics. *Anesth Analg* **92**:1182-1191.

Jenkins A, Greenblatt EP, Faulkner HJ, Bertaccini E, Light A, Lin A, Andreasen A, Viner A, Trudell JR and Harrison NL (2001) Evidence for a common binding cavity for three general anesthetics within the GABAA receptor. *J Neurosci* **21**:RC136(1-4).

Johansson JS and Zou H (1999) Partitioning of four modern volatile general anesthetics into solvents that model buried amino acid side-chains. *Biophys Chem* **79**:107-116.

Kemp JA and McKernan RM (2002) NMDA receptor pathways as drug targets. *Nat Neurosci* **5 Suppl**:1039-1042.

Koblin DD, Fang Z, Eger EI, 2nd, Laster MJ, Gong D, Ionescu P, Halsey MJ and Trudell JR (1998) Minimum alveolar concentrations of noble gases, nitrogen, and sulfur hexafluoride in rats: helium and neon as nonimmobilizers (nonanesthetics). *Anesth Analg* **87**:419-424.

Liu R, Pidikiti R, Ha CE, Petersen CE, Bhagavan NV and Eckenhoff RG (2002) The role of electrostatic interactions in human serum albumin binding and stabilization by halothane. *J Biol Chem* **277**:36373-36379.

Manderson GA and Johansson JS (2002) Role of aromatic side chains in the binding of volatile general anesthetics to a four-alpha-helix bundle. *Biochemistry* **41**:4080-4087.

Mascia MP, Machu TK and Harris RA (1996) Enhancement of homomeric glycine receptor function by long-chain alcohols and anaesthetics. *Br J Pharmacol* **119**:1331-1336.

Massey GM and Jackson SR (1973) Clinical anaesthesia with hexafluorobenzene in the dog. *Anaesthesia* **28**:327-230.

Mecozzi S, West AP, Jr. and Dougherty DA (1996) Cation-pi interactions in aromatics of biological and medicinal interest: electrostatic potential surfaces as a useful qualitative guide. *Proc Natl Acad Sci U S A* **93**:10566-10571.

Meyer H (1899) Theorie der alkoholnarkose. *Arch Exp Pathol Phamakol* **42**:109-118.

Mihic SJ, McQuilkin SJ, Eger EI, 2nd, Ionescu P and Harris RA (1994) Potentiation of gamma-aminobutyric acid type A receptor-mediated chloride currents by novel halogenated compounds correlates with their abilities to induce general anesthesia. *Mol Pharmacol* **46**:851-857.

Moss GW, Curry S, Franks NP and Lieb WR (1991) Mapping the polarity profiles of general anesthetic target sites using n-alkane-(alpha, omega)-diols. *Biochemistry* **30**:10551-10557.

Neal MJ and Robson JM (1966) The analgesic and anaesthetic actions of tetrafluorobenzene. *Br J Pharmacol* **26**:482-493.

Orser BA, Pennefather PS and MacDonald JF (1997) Multiple mechanisms of ketamine blockade of N-methyl-D-aspartate receptors. *Anesthesiology* **86**:903-917.

Overton E (1901) *Studien uber die narkose zugleich ein beitrag zur allgemein pharmakologie*, Jena.

Peoples RW and Ren H (2002) Inhibition of N-methyl-D-aspartate receptors by straight-chain diols: implications for the mechanism of the alcohol cutoff effect. *Mol Pharmacol* **61**:169-176.

Peoples RW and Weight FF (1995) Cutoff in potency implicates alcohol inhibition of N-methyl-D-aspartate receptors in alcohol intoxication. *Proc Natl Acad Sci U S A* **92**:2825-2829.

Peoples RW, White G, Lovinger DM and Weight FF (1997) Ethanol inhibition of N-methyl-D-aspartate-activated current in mouse hippocampal neurones: whole-cell patch-clamp analysis. *Br J Pharmacol* **122**:1035-1042.

Raines DE, Claycom RJ, Scheller M and Forman SA (2001) Nonhalogenated Alkane Anesthetics Fail to Potentiate Agonist Actions on Two Ligand-Gated Ion Channels. *Anesthesiology* **95**:470-477.

Raines DE and Claycomb RJ (2002) The role of electrostatic interactions in governing anesthetic action on the torpedo nicotinic acetylcholine receptor. *Anesth Analg* **95**:356-361.

Raines DE, Claycomb RJ and Forman SA (2002) Nonhalogenated anesthetic alkanes and perhalogenated nonimmobilizing alkanes inhibit alpha(4)beta(2) neuronal nicotinic acetylcholine receptors. *Anesth Analg* **95**:573-577.

Raines DE, Claycomb RJ and Forman SA (2003) Modulation of GABA(A) receptor function by nonhalogenated alkane anesthetics: the effects on agonist enhancement, direct activation, and inhibition. *Anesth Analg* **96**:112-118.

Sonner JM, Li J and Eger EI (1998) Desflurane and the nonimmobilizer 1,2-dichlorohexafluorocyclobutane suppress learning by a mechanism independent of the level of unconditioned stimulation. *Anesth Analg* **87**:200-205.

Tang P, Eckenhoff RG and Xu Y (2000) General anesthetic binding to gramicidin A: the structural requirements. *Biophys J* **78**:1804-1809.

Watts A (2002) Direct studies of ligand-receptor interactions and ion channel blocking (Review). *Mol Membr Biol* **19**:267-275.

Wick MJ, Mihic SJ, Ueno S, Mascia MP, Trudell JR, Brozowski SJ, Ye Q, Harrison NL and Harris RA (1998) Mutations of gamma-aminobutyric acid and glycine receptors change alcohol cutoff: evidence for an alcohol receptor? *Proc Natl Acad Sci U S A* **95**:6504-6509.

Wood SC, Forman SA and Miller KW (1991) Short chain and long chain alkanols have different sites of action on nicotinic acetylcholine receptor channels from Torpedo. *Molecular Pharmacology* **39**:332-338.

Wood SC, Hill WA and Miller KW (1993) Cycloalkanemethanols discriminate between volume- and length-dependent loss of activity of alkanols at the Torpedo nicotinic acetylcholine receptor. *Molecular Pharmacology* **44**:1219-1226.

Yamakura T and Harris RA (2000) Effects of gaseous anesthetics nitrous oxide and xenon on ligand-gated ion channels: comparison with isoflurane and ethanol. *Anesthesiology* **93**:1095-1101.

Zacharias N and Dougherty DA (2002) Cation-pi interactions in ligand recognition and catalysis. *Trends Pharmacol Sci* **23**:281-287.

Zhang Y, Trudell JR, Mascia MP, Laster MJ, Gong DH, Harris RA and Eger EI (2000) The anesthetic potencies of alkanethiols for rats: relevance to theories of narcosis. *Anesth Analg* **91**:1294-1299.

Zhong W, Gallivan JP, Zhang Y, Li L, Lester HA and Dougherty DA (1998) From ab initio quantum mechanics to molecular neurobiology: a cation-pi binding site in the nicotinic receptor. *Proc Natl Acad Sci U S A* **95**:12088-12093.

Zimmerman SA, Jones MV and Harrison NL (1994) Potentiation of gamma-aminobutyric acidA receptor Cl- current correlates with in vivo anesthetic potency. *J Pharmacol Exp Ther* **270**:987-991.

Footnotes

This work was supported by the National Institutes of Health GM61927 (to DER).

Portions of this work were presented in abstract form at the annual meeting of the American Society of Anesthesiologists, San Francisco, CA (2003).

Address correspondence to Douglas E. Raines, Department of Anesthesia and Critical Care, Massachusetts General Hospital, 55 Fruit Street, Boston, MA 02114

Legends for Figures

Figure 1: Inhibition of human N21/NR2B NMDA receptors by aromatic inhalants. Representative current traces in the presence of benzene (A), 1,3,5-trifluorobenzene (B), and perfluorobenzene (C). In figures 1A, 1B, and 1C, the first and last traces are the control currents recorded upon pulsing *Xenopus* oocytes expressing NR1/NR2B NMDA receptors with agonist and the middle trace demonstrates the inhibitory action of the inhalant. Figure 1D shows the inhalant concentration-current response curves for benzene, 1,3,5-trifluorobenzene, and perfluorobenzene. Each point is the mean of at least three measurements using three different oocytes and the errors bars indicate the standard deviations. The curves are the best fits of the data to equation 2 and the results of these fits are given in table 1.

Figure 2: Correlation between the NMDA receptor inhibitory potencies of aromatic inhalants and their oil:gas partition coefficients (A) or molecular volumes (B). In each figure, the line was derived from linear least-squares analysis. (A) r^2=0.30 and p = 0.044; (B) p = 0.14 and r^2=0.19.

Figure 3: The electrostatic potential surfaces of aromatic inhalants and their cation-π interaction strengths. Geometry optimization was performed using *ab initio* molecular orbital calculations (Hartree-Fock, 6-31G** basis set). The cation-π binding energy was defined as the negative binding energy of a generic cation probe (Na^+) to each inhalant's π electron cloud as previously described (Mecozzi et al., 1996). A color scale ranging from +20 to –20 kcal/mol to emphasize the electrostatic potential

differences in the aromatic ring regions. Blue was used to signify an electrostatic potential equal to or more positive than +20 kcal/mol and red to indicate a potential equal to or more negative than –20 kcal/mol.

Figure 4: Correlation between the NMDA receptor inhibitory potencies of aromatic inhalants and their abilities to engage in cation-π interactions. The line was derived from linear least-squares analysis. There is a strong correlation between an inhalant's NMDA receptor inhibitory potency and its ability to engage in a cation-π interaction ($r^2 = 0.85$, $p < 0.0001$).

Figure 5: Correlation between the NMDA receptor inhibitory potencies of volatile compounds and their abilities to engage in cation-π interactions (A), oil:gas partition coefficients (B), or molecular volumes (C). In each figure, the line was derived from linear least-squares analysis. (A) r^2=0.97 and p = 0.0004; (B) r^2=0.22 and p = 0.355; (C) r^2=0.14 and p = 0.86.

Figure 6: Inhibition of NMDA receptors by benzene or perfluorobenzene does not vary with NMDA or glycine concentrations. The data represent the mean and standard deviations obtained using 5 oocytes. Currents were measured upon activation by 100 μM NMDA and 10 μM glycine, 1000 μM NMDA and 10 μM glycine, or 100 μM NMDA and 100 μM glycine.

JPET Fast Forward. Published on May 27, 2004 as DOI: 10.1124/jpet.104.069930
This article has not been copyedited and formatted. The final version may differ from this version.

Table 1: Partition Coefficients, NMDA Receptor IC_{50}s, and Molecular Volumes of Volatile Aromatic Inhalants. Data are presented as mean ± S.D.

Inhalant	$\lambda_{buffer:gas}$	$\lambda_{octanol:gas}$	IC_{50} (atm)*	Hill Coefficient	Molecular Volume ($Å^3$)
Benzene	4.9 ± 0.3	940 ± 50	$1.1 \pm 0.1 \times 10^{-3}$	1.2 ± 0.1	86.6
Toluene	4.8 ± 0.3	1830 ± 110	$5.6 \pm 0.3 \times 10^{-4}$	1.0 ± 0.1	103.8
o-Xylene	7.0 ± 1.0	9860 ± 300	$7.8 \pm 0.4 \times 10^{-4}$	0.82 ± 0.1	119.6
m-Xylene	4.1 ± 0.2	8430 ± 400	$1.9 \pm 0.2 \times 10^{-3}$	0.67 ± 0.06	119.7
p-Xylene	3.0 ± 0.7	5300 ± 210	$7.4 \pm 1.1 \times 10^{-4}$	0.72 ± 0.04	119.7
Ethylbenzene	3.5 ± 0.1	5450 ± 310	$1.1 \pm 0.2 \times 10^{-3}$	0.75 ± 0.10	119.8
Fluorobenzene	4.7 ± 0.3	930 ± 70	$8.1 \pm 0.6 \times 10^{-4}$	0.96 ± 0.06	92.1
o-Difluorobenzene	4.7 ± 0.2	1290 ± 130	$8.8 \pm 0.8 \times 10^{-4}$	0.94 ± 0.05	97.6
p-Difluorobenzene	4.4 ± 0.2	1230 ± 80	$4.8 \pm 0.2 \times 10^{-3}$	1.5 ± 0.1	97.6
1,3,5-Trifluorobenzene	2.1 ± 0.3	520 ± 40	$5.1 \pm 0.5 \times 10^{-3}$	1.0 ± 0.1	103.0
1,2,4-Trifluorobenzene	2.8 ± 0.6	950 ± 60	$5.9 \pm 0.8 \times 10^{-3}$	0.8 ± 0.1	101.0
Pentafluorotoluene	1.0 ± 0.1	1970 ± 50	$3.4 \pm 0.9 \times 10^{-2}$	1.0 ± 0.2	128.1
Pentafluorobenzene	1.1 ± 0.1	640 ± 10	$4.3 \pm 0.1 \times 10^{-2}$	1.0 ± 0.1	114.0
Perfluorobenzene	0.84 ± 0.03	390 ± 10	$9.2 \pm 0.8 \times 10^{-2}$	0.75 ± 0.04	119.4

* IC_{50} (atm) = IC_{50} (mM)/[(44.614)($\lambda_{buffer:gas}$)]

Figure 1

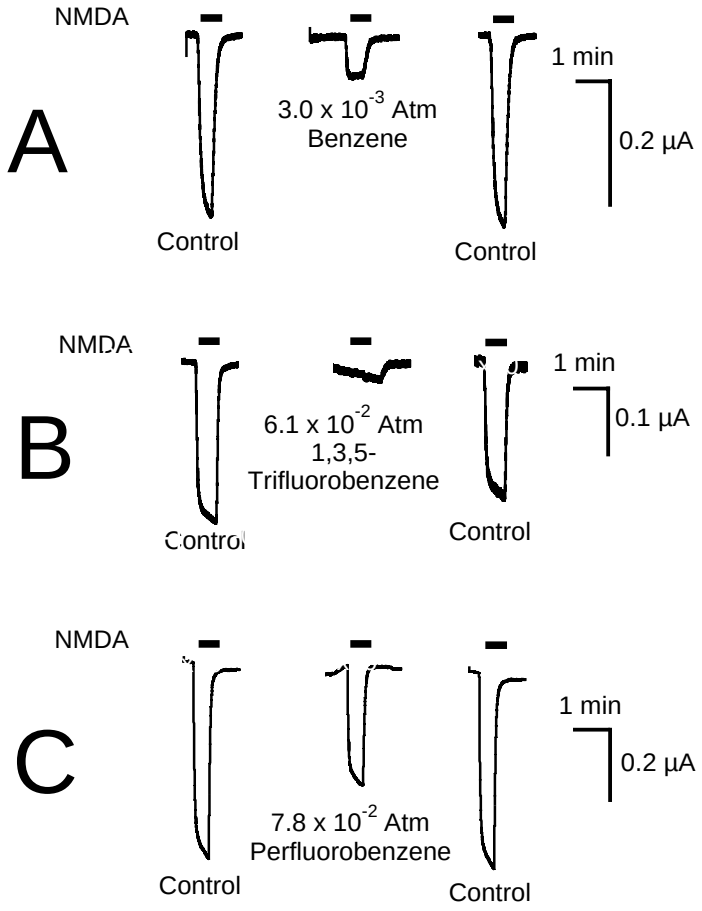

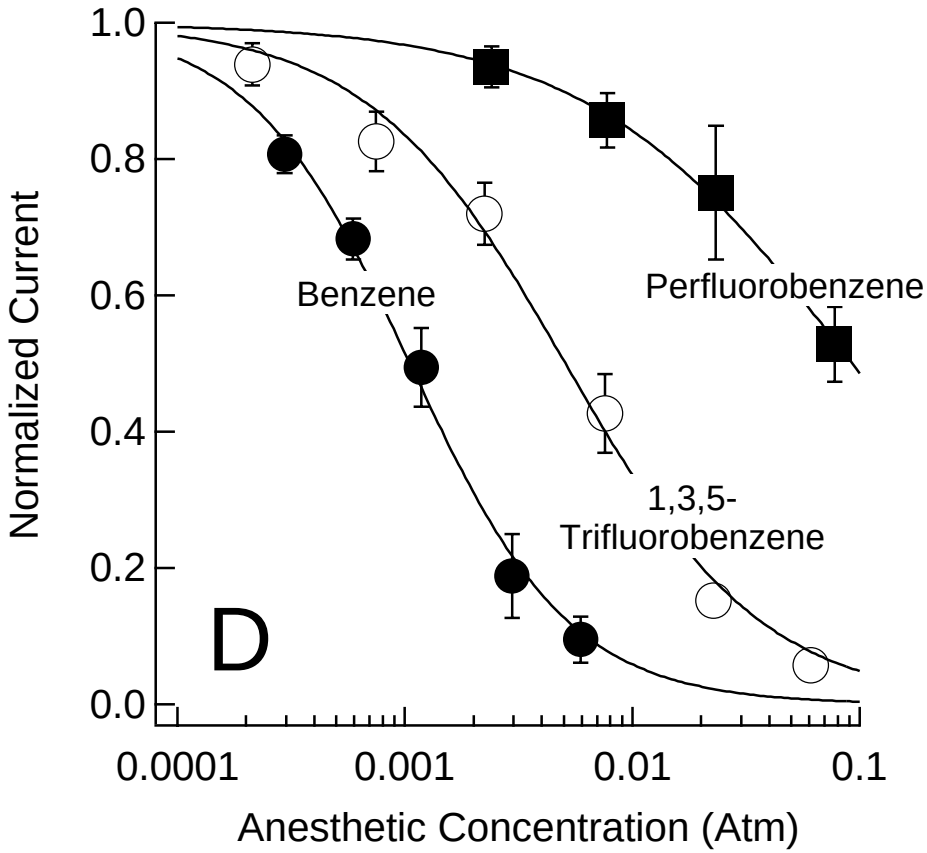

Figure 2

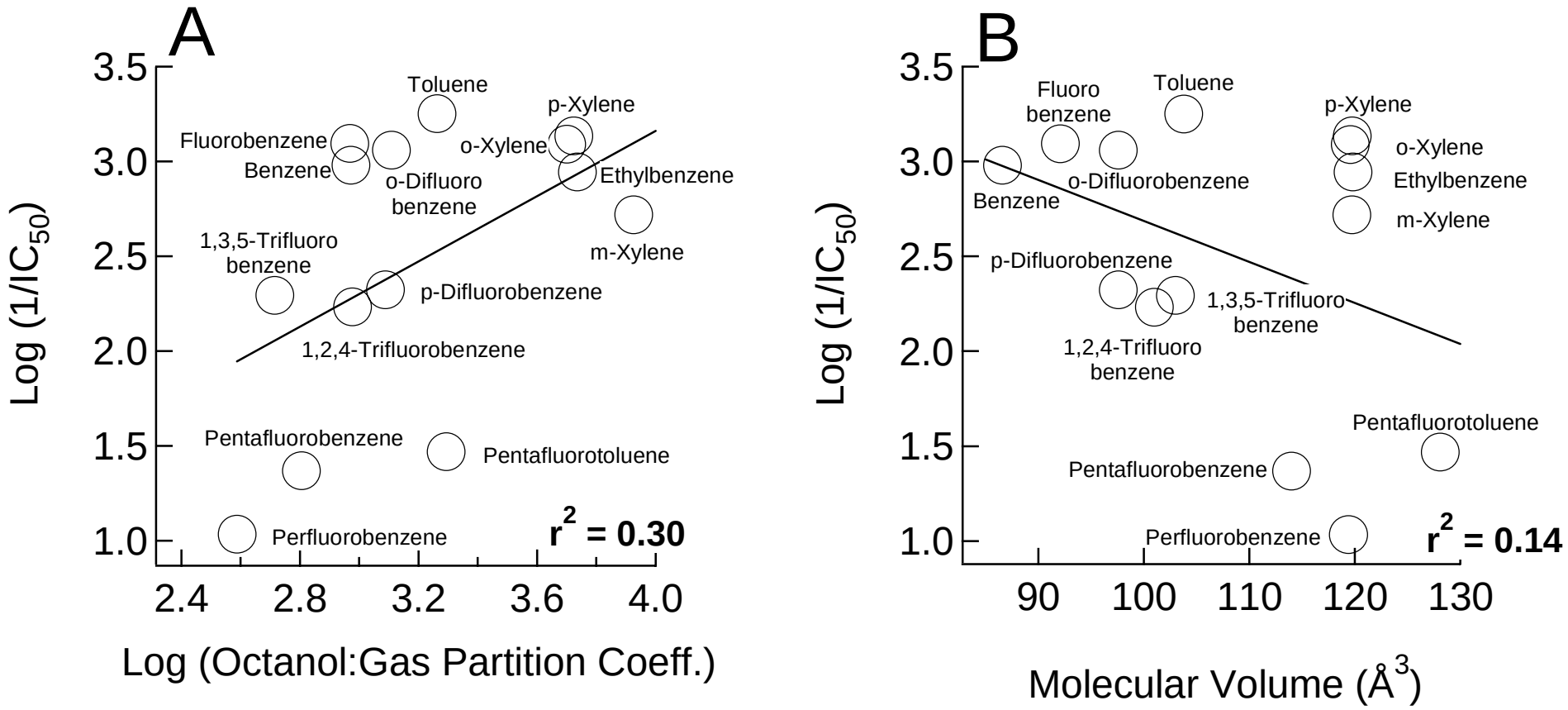

JPET Fast Forward. Published on May 27, 2004 as DOI: 10.1124/jpet.104.069930
This article has not been copyedited and formatted. The final version may differ from this version.

Figure 3

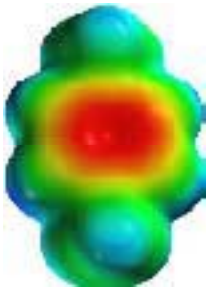

p-Xylene
29.7

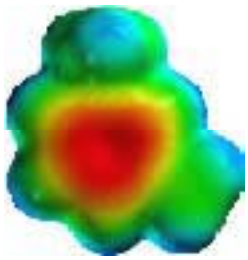

m-Xylene
29.7

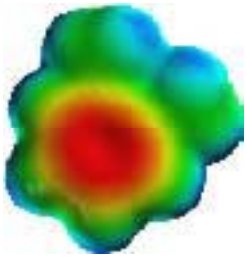

o-Xylene
29.3

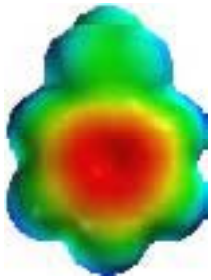

Ethylbenzene
28.8

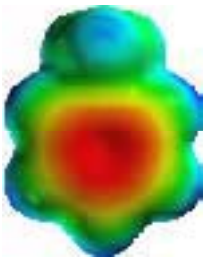

Toluene
28.6

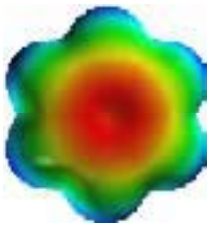

Benzene
27.1

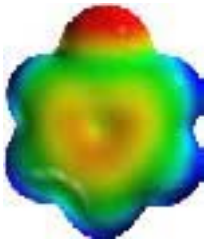

Fluorobenzene
22.0

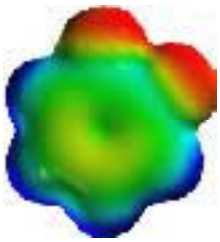

o-Difluoro-
benzene
17.4

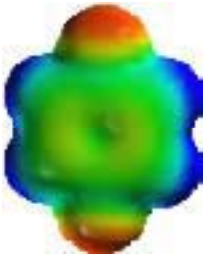

p-Difluoro-
benzene
16.8

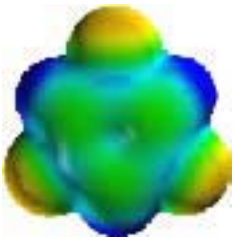

1,3,5-Trifluoro-
benzene
13.7

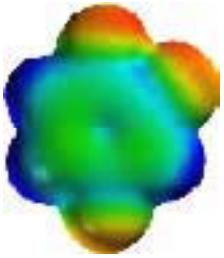

1,2,4-Trifluoro-
benzene
13.7

Pentafluoro-
toluene
5.7

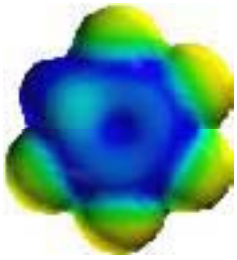

Pentafluoro-
benzene
3.9

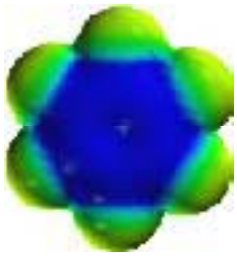

Perfluoro-
benzene
0.0

JPET Fast Forward. Published on May 27, 2004 as DOI: 10.1124/jpet.104.069930
This article has not been copyedited and formatted. The final version may differ from this version.

Figure 4

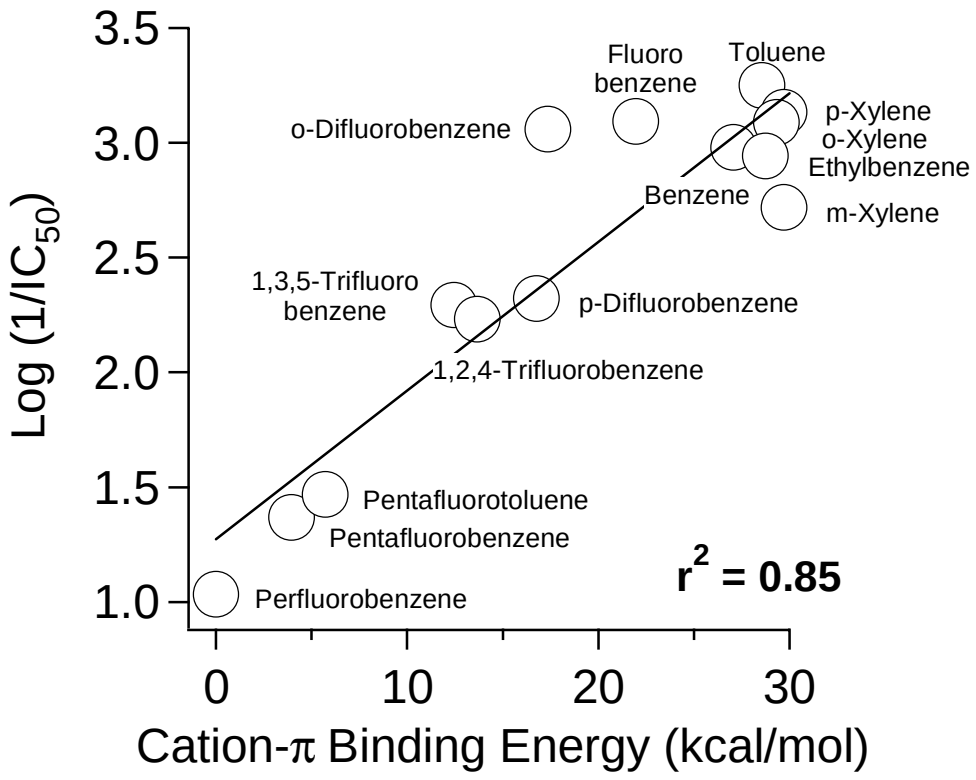

Figure 5